AD-A070 630 AMERICAN UNIV WASHINGTON D C F/G 20/1
ROUGH SURFACE ACOUSTIC SCATTERING AND SCATTERING OF ACOUSTIC WA--ETC(U)
APR 79 S K NUMRICH, E CALLEN N00014-77-C-0142
UNCLASSIFIED NL

| OF |
AD
A070630

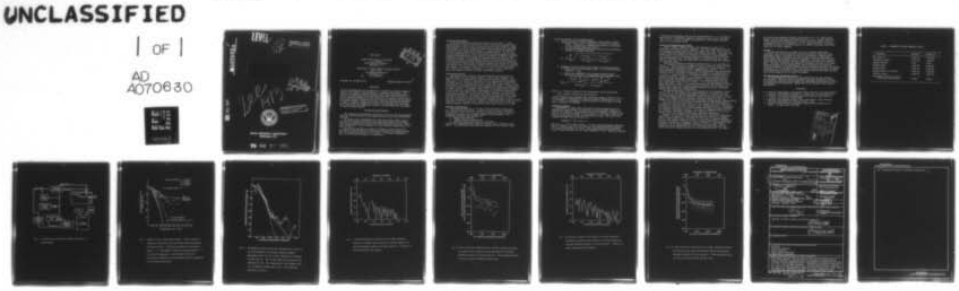

END
DATE
FILMED
8 -79
DDC

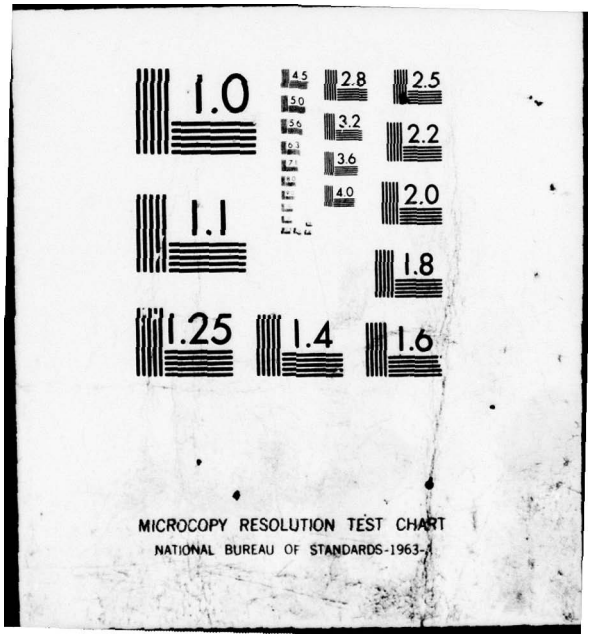
1.0
1.1
1.25
1.4
1.6
1.8
2.0
2.2
2.5
2.8
3.2
3.6
4.0
4.5
5.0
5.6
MICROCOPY RESOLUTION TEST CHART
NATIONAL BUREAU OF STANDARDS-1963-A

LEVEL II

12
P.S.

ENCLOSURE (3) TO NRL
LETTER 8132-71:SKN:jw
OF

AD A070630

DDC
RECEIVED
JUN 27 1979
C

DDC FILE COPY

1417

This document has been approved for public release and sale; its distribution is unlimited.

NAVAL RESEARCH LABORATORY
Washington, D.C.

79 06 27 004

Final Report

Rough Surface Acoustic Scattering
S. K. Numrich
Naval Research Laboratory
Washington, D.C.

Scattering of Acoustic Waves from Rough Surfaces
Earl Callen
The American University
Washington, D.C.
and S. K. Numrich

WORK UNIT NO. NR RR032-05-01 CONTRACT N00014-77-C-0142

OBJECTIVES

(a) The long range goal of the research is to provide an accurate parameterization of the acoustic field scattered by a randomly rough surface. The research is designed to evaluate existing rough surface scattering models in view of their application to scattering from the under surface of the ice. (b) The immediate objectives of this problem are to construct random surfaces with surface height distributions that are measurably Gaussian and have known correlation lengths; display the acoustic field scattered from the surface by means of schlieren visualization; measure the scattered field with underwater transducers; and compare the results to existing models for scattering of sound by random surfaces.

ACTIVITIES/ACCOMPLISHMENTS

The investigations undertaken through both the task at the Naval Research Laboratory and the contract at The American University have been successfully completed.

Two rough surface topographies were constructed under computer control to have surface height distributions and slope distributions that differed from Gaussian statistics by no more than 0.0036 (mean squared error). Table I lists the principal surface parameters for both surfaces. Rough surface I is shown in Fig. 1.

Each surface was used in a series of underwater acoustic scattering measurements which employed three different experimental techniques to determine the scattering properties of the surface. The geometry diagrammed in Fig. 2 was maintained throughout all experiments.

Schlieren Visualization.

A typical schlieren visualization system is shown in Fig. 3. This method was used to provide a qualitative view of the entire scattered field. The photographs in Fig. 4 show a 1 MHz pulse directed down toward the target, rough surface I. As the transducer moves across the surface the sound pulse is scattered from various surface features. The pictures of the scattered field (B, C and D) change as the surface topography changes. In each case the area insonified was at least three surface correlation lengths in extent. Insonifying different parts of the surface corresponds to sampling a different population (in this case of height and slope distributions) from the same statistical ensemble. The predominant features in all visualizations of the scattered field are the angular diffusion of the sound due to the orientation of the surface's slopes and the interference pattern that results when returns from various parts of the surface interfere destructively because of differing path lengths. The scattered field in Fig. 4 is the total field containing both coherent and incoherent components. For surface I and a 1 MHz sound pulse, the coherent term which includes interference dominates.

Steady State Analysis.

Experiments in microacoustics have traditionally used long pulses to make measurements at the resonant frequency of the source transducer. The signal is read far enough into the pulse (in time) to make transient effects unimportant. The reflection coefficient for the rough surface is determined by normalizing the scattered return with a return from a flat surface of the same material at the same distance from the source and receiver. Figure 5 shows reflection coefficients measured at two frequencies by steady state techniques for rough surface I. The geometry shown in Fig. 2 is retained as the transducer is moved across the rough surface. Measurements of the sound scattered back to the receiver were made at thirty-one discrete locations. The reflection coefficients computed for these points are joined to provide the solid curves displayed in the figure. (At normal incidence, scattering back at the source is a case of specular scattering rather than of backscattering.) As with schlieren visualization, there is no means to separate the coherent and incoherent components of the scattered field. However, at both 1 MHz and 2.25 MHz the coherent component dominates the scattered field, albeit less so at 2.25 MHz.

Transient Pulse Analysis.

This technique makes use of the most recent advances in microacoustic data acquisition and processing. A pulser is used to trigger a transducer. This generates a short (1.5-3.5 cycle) pulse containing a broad spectrum of frequencies centered on the resonant frequency of the transducer. The experimental procedure used consisted of

1. sampling the waveform,
2. taking a Fourier transform, and
3. computing the desired reflection coefficient.

A series of 31 measurements were taken at different places along the rough surface. The reflection coefficients were computed for the different terms

(total and coherent) in the following ways:

1. Total (includes all energy regardless of path length or phase)
   a. Normalize each of the 31 samples by the proper flat surface return. (Equivalent to computing the reflection coefficient for each position along the surface.)
   b. Average the normalized reflection coefficients and determine the mean and standard deviation.

$$R_T = \frac{1}{N} \sum_{i=1}^{N} \sqrt{\frac{[\text{Re}(p_{si})]^2 + [\text{Im}(p_{si})]^2}{[\text{Re}(p_{ref})]^2 + [\text{Im}(p_{ref})]^2}}$$

2. Coherent (retains the phase term through the averaging process)
   a. Average the real and imaginary parts of the scattered returns separately. (P_{si})
   b. Compute the magnitude of this average scattered return.
   c. Normalize the result by the magnitude of the reference pulse.

$$R_{COH} = \sqrt{\frac{\frac{1}{N}\left[\text{Re}\left(\sum_{i=1}^{N} p_{si}\right)\right]^2 + \frac{1}{N}\left[\text{Im}\left(\sum_{i=1}^{N} p_{si}\right)\right]^2}{[\text{Re}(p_{ref})]^2 + [\text{Im}(p_{ref})]^2}}$$

where P_{si} = Pressure scattered by the rough surface at the ith position

P_{ref} = Pressure reflected by smooth surface.

A block diagram of the transient pulse acquisition scheme is shown in Fig. 6. By using several transducers with different resonant frequencies (0.5, 1.0, 2.25, 5.0 MHz) it was possible to span frequencies from 0.14 MHz to 8.0 MHz with a resolution of 0.025 MHz.

Roughness Parameter.

Comparisons in rough surface scattering are made through the use of a dimensionless factor known as the Rayleigh roughness parameter (referred to herewith as roughness). This parameter scales the roughness according to the ratio of the surface rms height to the wavelength of the sound. This is then modified by the angle at which the measurements are made. The form of the roughness parameter used in the work is

$$\text{Roughness} = \frac{2\pi}{\lambda} \sigma \cos \theta_i = \Sigma$$

where $\cos \theta_i = 1$ for normal incidence. In recent years measurements have been made for roughness less than 3.0; however, only measurements below roughness of 1.5 were in agreement with theory. Radar measurements characterized the largely incoherent energy for very large roughness ($\sim$ 10.0). Relative influences

of coherent and incoherent terms in the region between $2.0 < \Sigma < 10.0$ had not been explored. Measurements completed through this task covered the region from $\Sigma = 0.2$ to ≥ 20.0, including the separation of the coherent component from the total scattered field.

Results and Comparisons with Theory.

Figure 7 shows a summary of theory and experiment in terms of the reflection coefficient for small roughness. Both the DeSanto theory and the characteristic function involve only the coherent term. This is also true of the experimental measurements done by Clay, Medwin and Wright. The solid curve marked as the total reflection coefficient was measured in this experiment. Its inclusion in this illustration indicates a possible difficulty with the Boyd and Deavenport data. Although assumed to be coherent, the data falls closer to the total reflection coefficient curve which includes both coherent and incoherent terms.

The coherent reflection coefficients measured for $\Sigma < 3.0$ are shown in Fig. 8. The smaller values of roughness (•) were achieved by using a 0.5 MHz transducer. The remaining measurement (x) employed a 5.0 MHz transducer. These measurements continue to values roughness greater than 20. At $\Sigma = 1.9$ the experimental measurements begin to differ significantly from theoretically predicted values. Excursions in magnitude that begin in the measurements at $\Sigma = 1.6$ are a characteristic of the coherent reflection coefficient as the roughness increases. At about $\Sigma = 2$ the interference of scattered returns having different path lengths becomes important. The measurements shown in Fig. 8 agree with theoretical predictions to a far greater extent than the Boyd and Deavenport data in Fig. 7. Below $\Sigma = 1.5$ the measurements should agree with theory. Above $\Sigma = 2.0$ where interference becomes important, neither theory should be able to accurately predict the behavior of the sound since neither theory takes into account phase differences and surface correlation lengths which contribute to interference.

The measurements shown in Fig. 8 are extended for the remainder of their range in Fig. 9. The presence of interference minima is characteristic for all large roughness, coherent measurements; however, the location and extent of the minima depend upon the particular surface features insonified. In other words, the scattered field for different statistical samples of the same ensemble will differ in some detail while retaining the same general characteristics.

The total reflection coefficients computed from the same measurements of the scattered field are shown in Fig. 10. The average value of the reflection coefficient is bracketed above and below by one standard deviation. The presence of incoherent terms which do not exhibit phase cancellation virtually eliminates any noticeable interference pattern. For values of roughness greater than 2.0, the incoherent term begins to dominate the reflection until at $\Sigma = 11.0$, the coherent term is 20 dB down from the total reflection coefficient.

Figures 11 and 12 present the coherent and total reflection coefficients, respectively, for surface I. Since the rms height of surface I is roughly a factor of three greater than for surface II, the range of roughness measured with the same acoustic sources is a factor of three larger with a corresponding decrease in resolution (in roughness, not in frequency). The dominance of the incoherent term at large roughness is evident in this case also. Direct comparisons can be made between the total reflection coefficients for both surfaces using the roughness parameter as the appropriate scale. The same is

not true for the coherent reflection coefficients at $\Sigma > 1.5$. This is the region in which path length interference begins to occur. Because individual surface features become important, the surface correlation length enters as a necessary factor in the comparison. If the roughness parameter is further normalized by surface correlation length, the coherent reflection coefficients agree even for large roughness.

Summary.

The NRL experiment has (a) begun in the low frequency region where comparisons with the characteristic curve would provide a validation of the measurement scheme, (b) spanned the region of intermediate roughness where previous data were questionable, and (c) provided scattering measurements at high roughness where previous data were inadequate. Both the total reflection coefficient and the coherent term were computed from the same set of measurements. Coherent coefficients are needed for comparison with many of the newer theoretical models and for assessing the relative importance of height and slope distributions, correlation lengths and source characteristics as controlling parameters in the scattering process. The total reflection coefficient is needed for application to a variety of practical problems, particularly those concerned with sound propagation in the Arctic environment.

Work Distribution Between NRL and A.U.

All experimental work was done at NRL together with the data analysis and reporting. Computer software and hardware developed through the contract at The American University made possible the comparisons with theoretical models and implemented the experimental design used in the transient pulse analysis measurements.

References

S. K. Numrich, "Measurement of the Acoustic Field Scattered at the Liquid-Solid Interface of an Echelette Grating," J. Acoust. Soc. Am. 60, S56(A) 1976.

S. K. Numrich, "Scattering of Acoustic Waves from Randomly Rough Surfaces," J. Acoust. Soc. Am. 64, S131(A) 1978.

S. K. Numrich, "Scattering of Acoustic Waves from Randomly Rough Surfaces," University Microfilms Int., Ann Arbor, Mich., 1979.

S. K. Numrich, "Rough Surface Scattering," Naval Research Laboratory 1978 Review. (in publication for 1979)

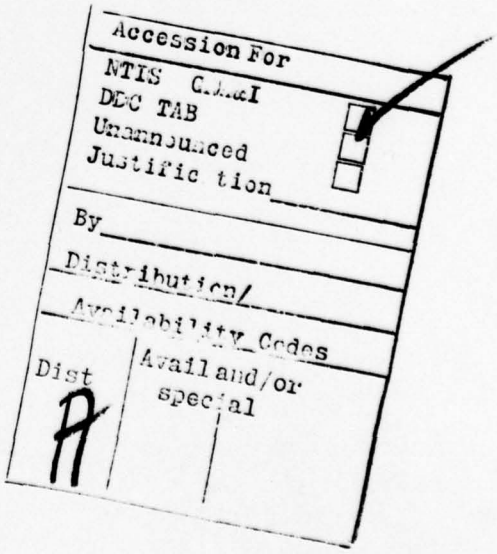

TABLE 1. PARAMETERS OF ROUGH SURFACES I AND II

Parameters	Surface I	Surface II
RMS height (σ)	0.124 CM	0.037 CM
Correlation Length	0.737 CM	0.305 CM
Maximum Gradiant	0.492	0.458
Maximum Height	0.238 CM	0.094 CM
Maximum Depth	-0.313 CM	-0.078 CM
Minimum Radius of Curvature	0.891 CM	0.328 CM
Milling Accuracy	0.005 CM	0.005 CM
Mean-Squared Deviation from the Theoretical Distribution	0.0036	0.0016

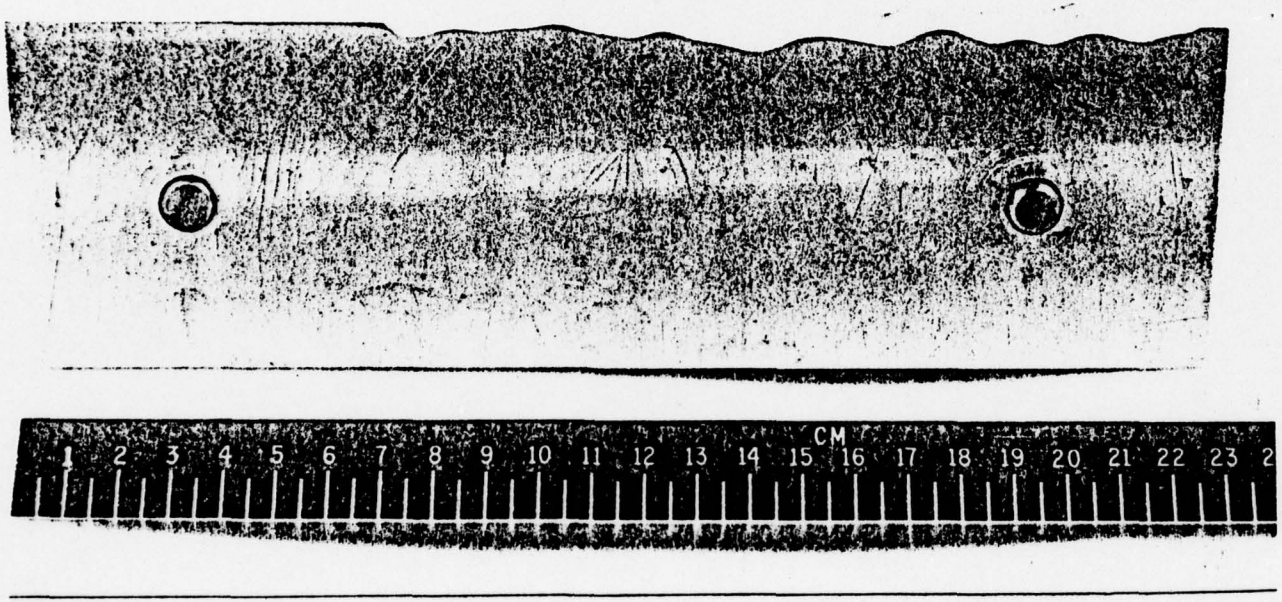

Fig. 1 Photograph of Surface I. The rms height is 0.124 cm with a 0.737 cm correlation length. The block is 25.4 x 7.6 x 7.6 cm. THe milled rough surface is 17.0 cm long.

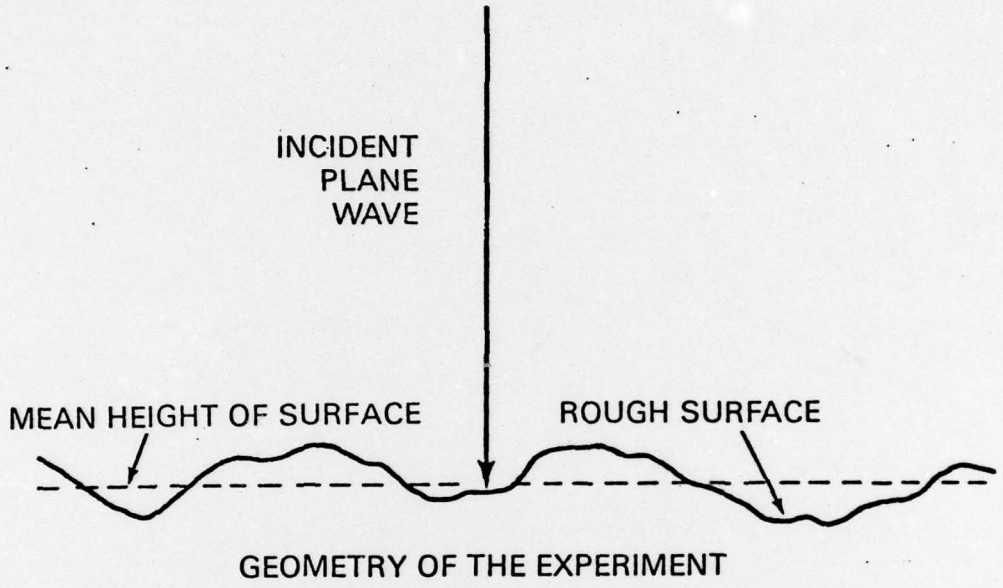

Fig. 2 The orientation of a source and surface for all the experiments is pictured. The sound was normally incident on the nominal mean of the surface.

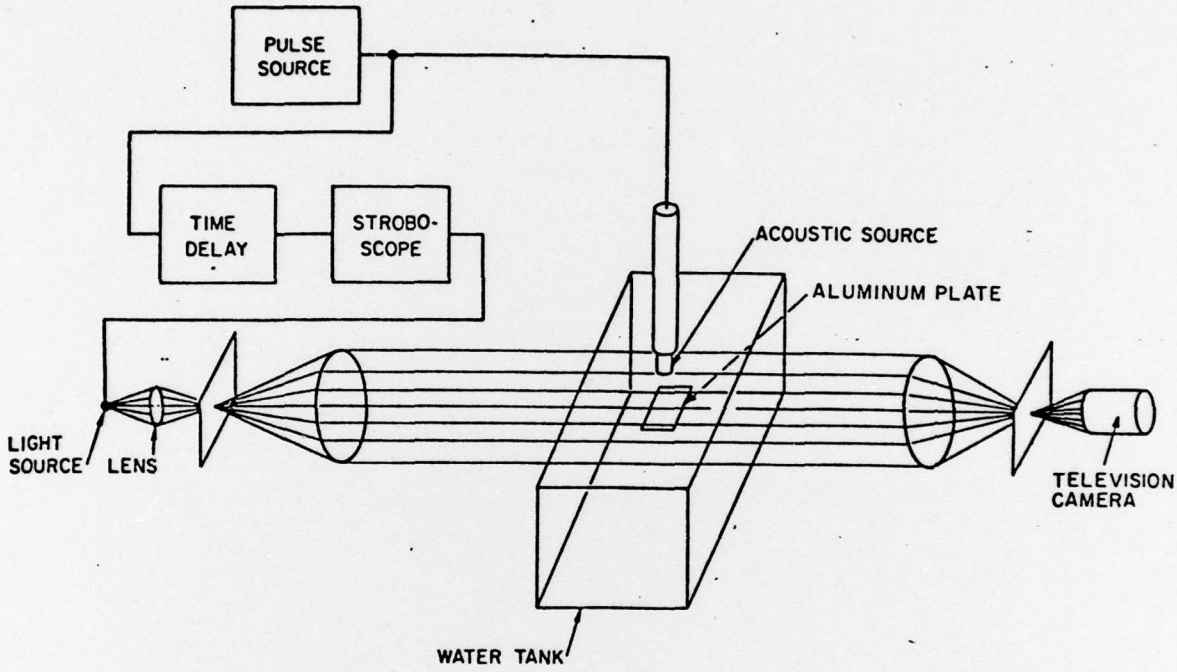

Fig. 3 A typical schlieren visualization system is shown as a block diagram. Disturbances in the water caused by the sound pressure produce an image at the camera lens.

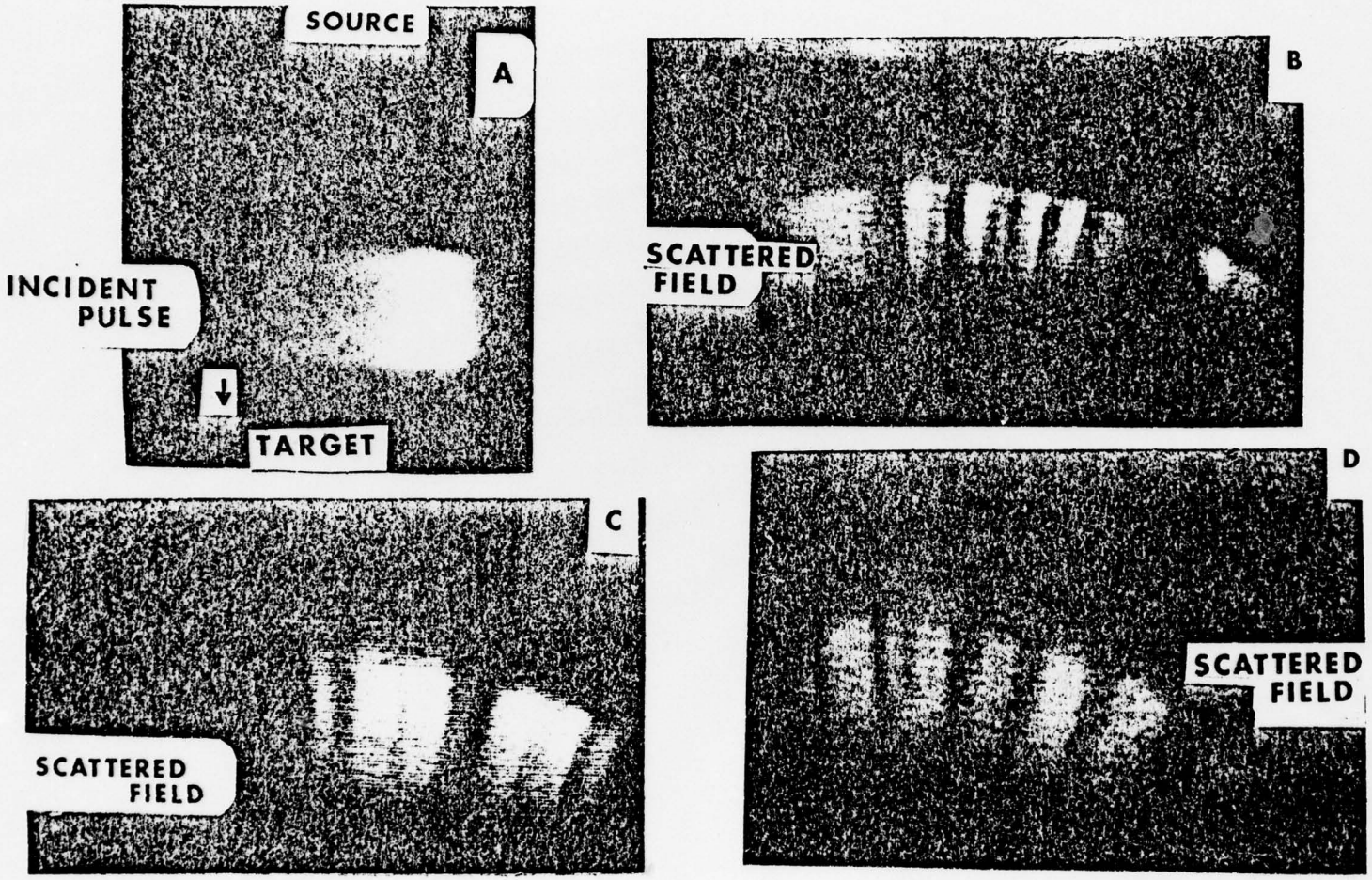

Fig. 4 Schlieren photographs of the incident and the scattered fields. The incident pulse is shown in (a). The scattered field in (b), (c),and (d) demonstrates the effects of phase cancellation.

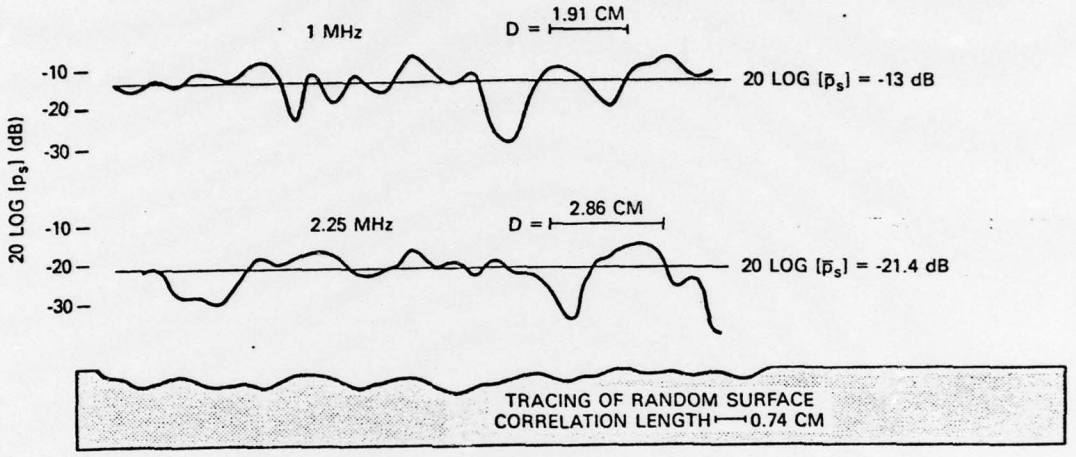

Fig. 5 Steady state pulse measurements are plotted for two frequencies. The reflection coefficients are shown above the section of the surface where they were measured. The transducer diameters and the surface topography (surface I) are drawn to scale.

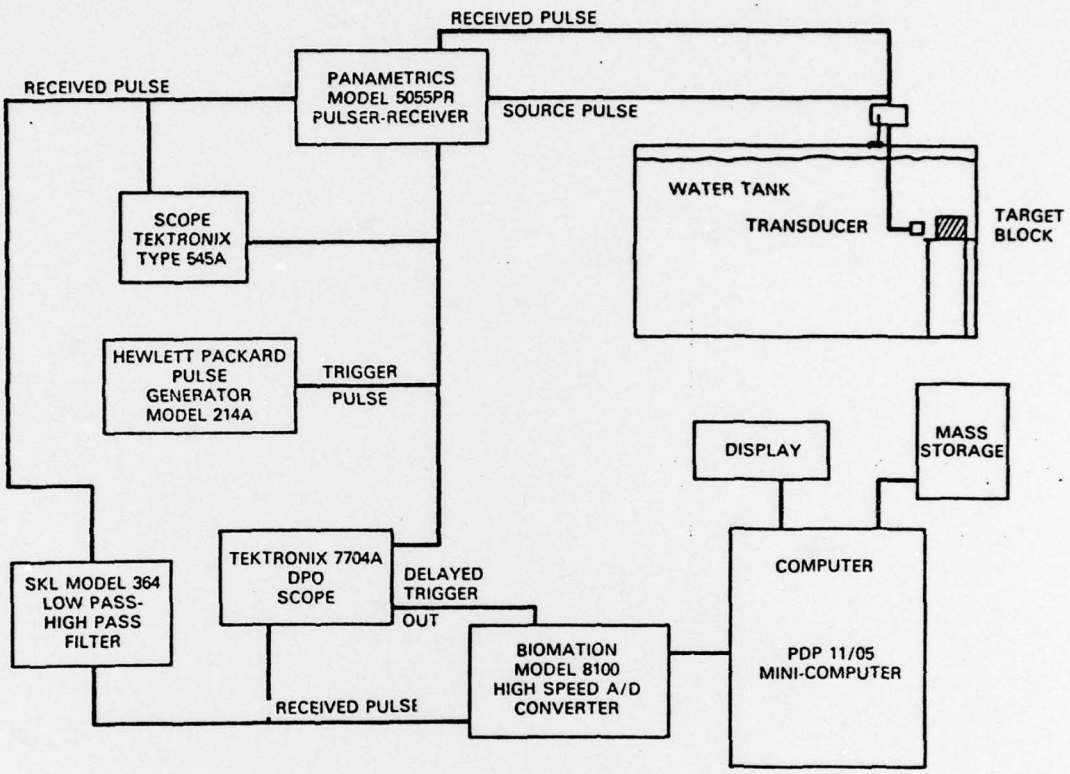

Fig. 6 Transient pulse acquisition scheme is shown as a block diagram.

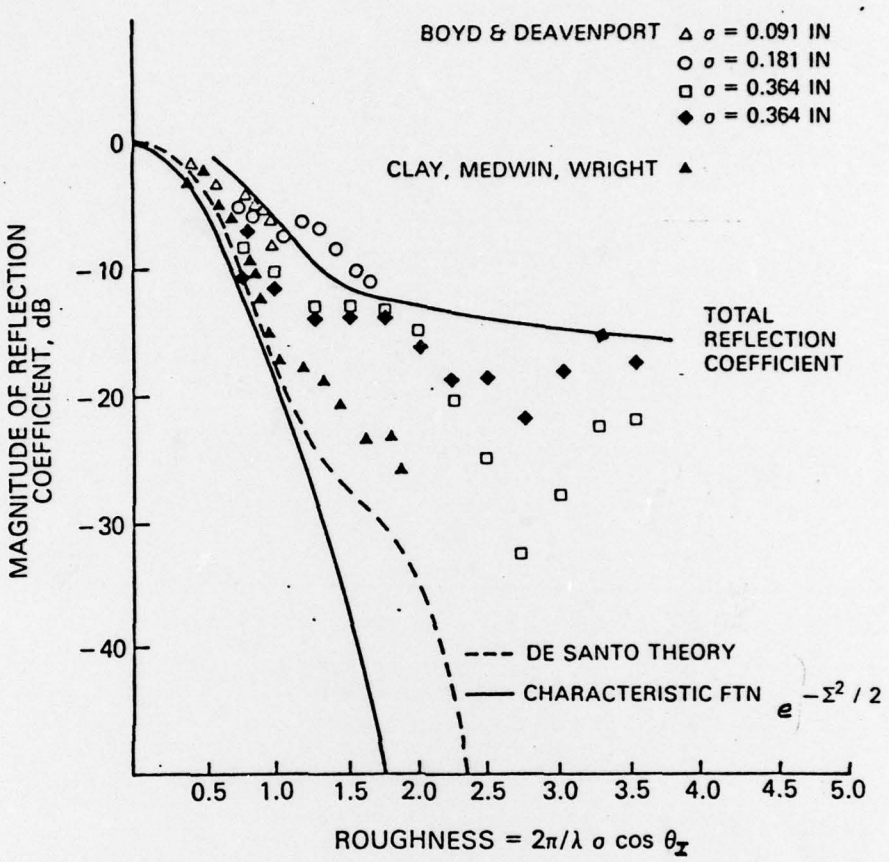

Fig. 7 Summary of major experimental results. Data for coherent reflection coefficients from wind-driven water surfaces, ▲, and fixed surfaces. Theoretical predictions from Eckart's theory, ———, and DeSanto's multiple scattering model, — — — , are shown for comparison. Total measured reflection coefficients computed in this experiment provide a comparison for the fixed surface data.

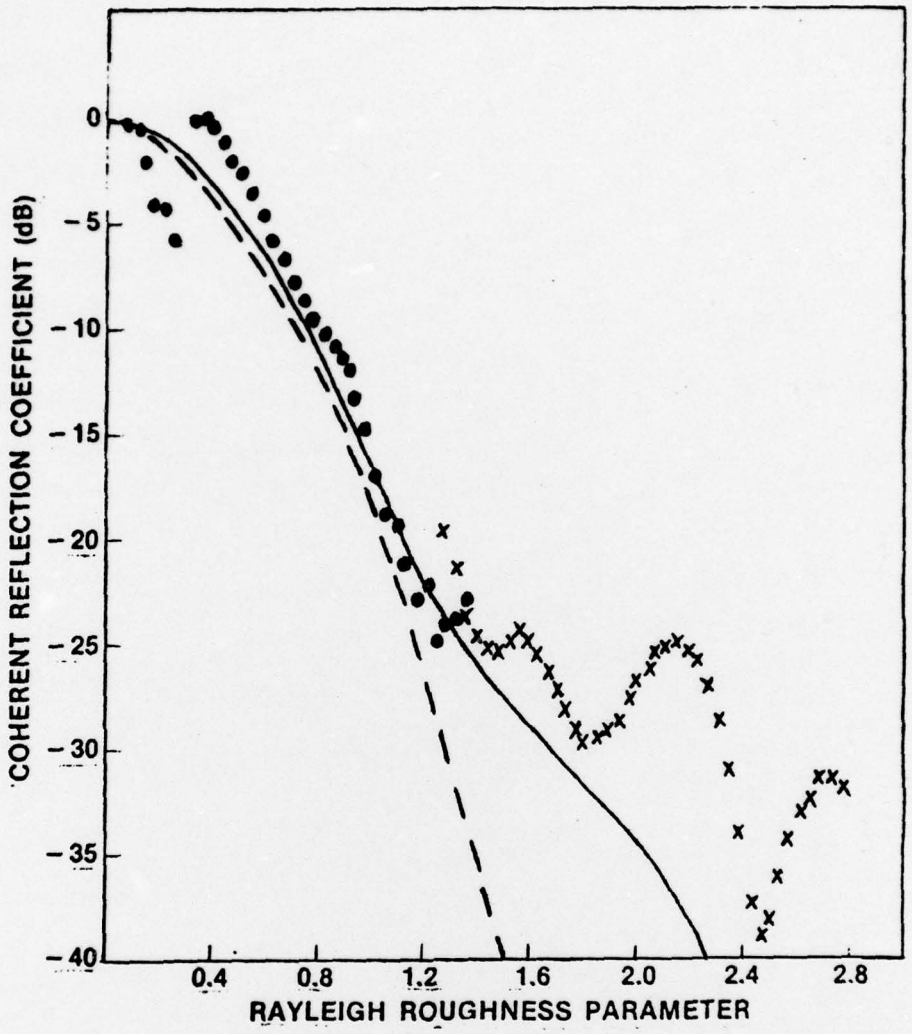

Fig. 8 The measured coherent reflection coefficients for surface II are plotted against the Rayleigh roughness parameter. Measurements made with the 0.5 MHz transducer are indicated by solid dots (•). The 5.0 MHz transducer was used for the remaining data (X). The characteristic curve (dashed curve ---) and DeSanto's model (solid curve —) are shown for comparison as in Fig. 7.

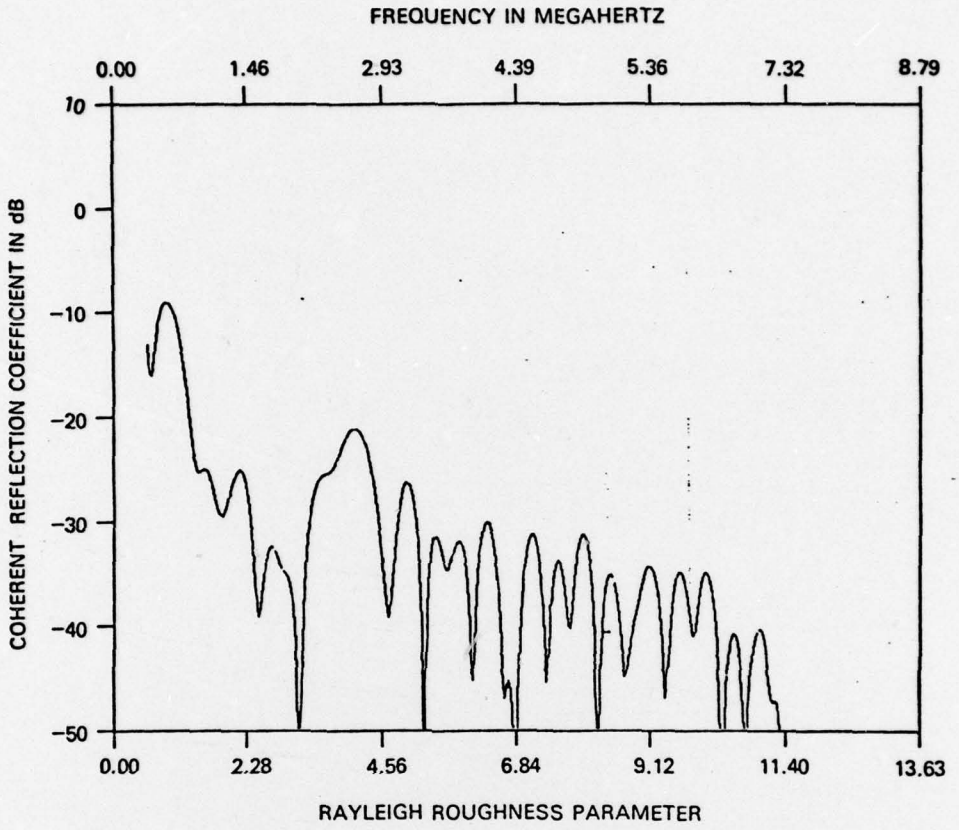

Fig. 9 Coherent Reflection coefficients for 5.0 MHz transducer obtained by transient pulse analysis are plotted against the Rayleigh foughness parameter for brass surface II. Effects of phase cancellation are dramatic.

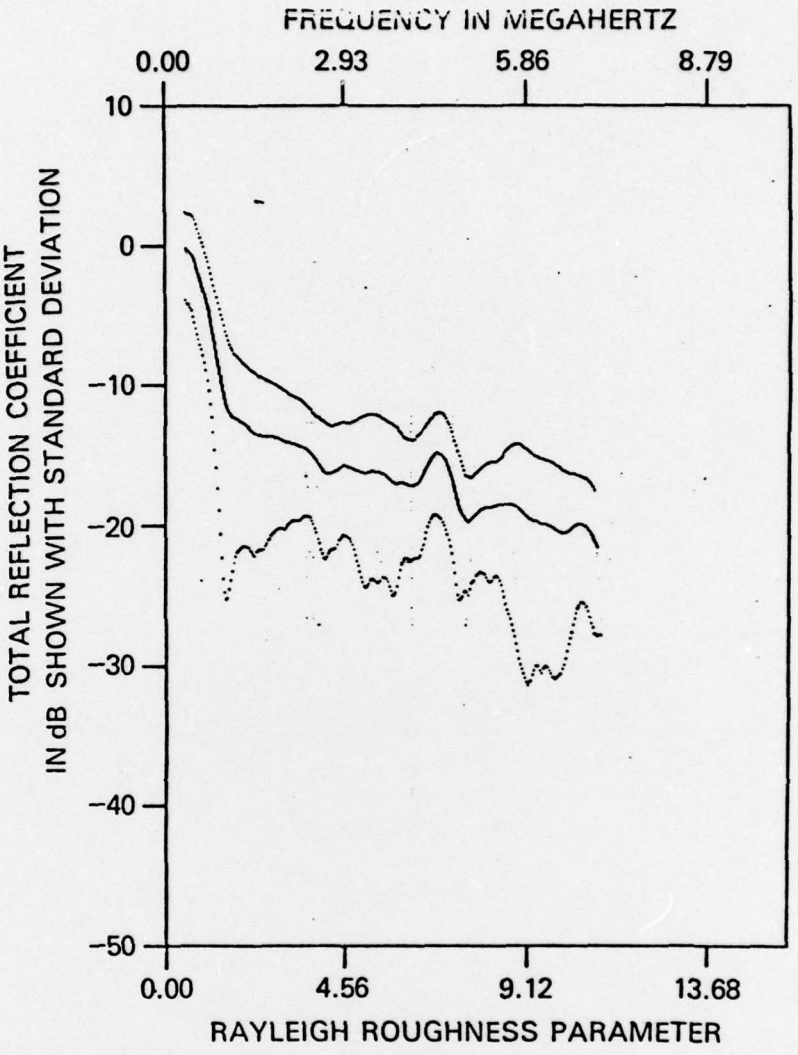

Fig. 10 Total reflection coefficients for 5.0 MHz transducer obtained by transient pulse analysis are plotted against the Rayleigh roughness parameter for brass surface II. The standard deviation for each data point brackets the mean curve.

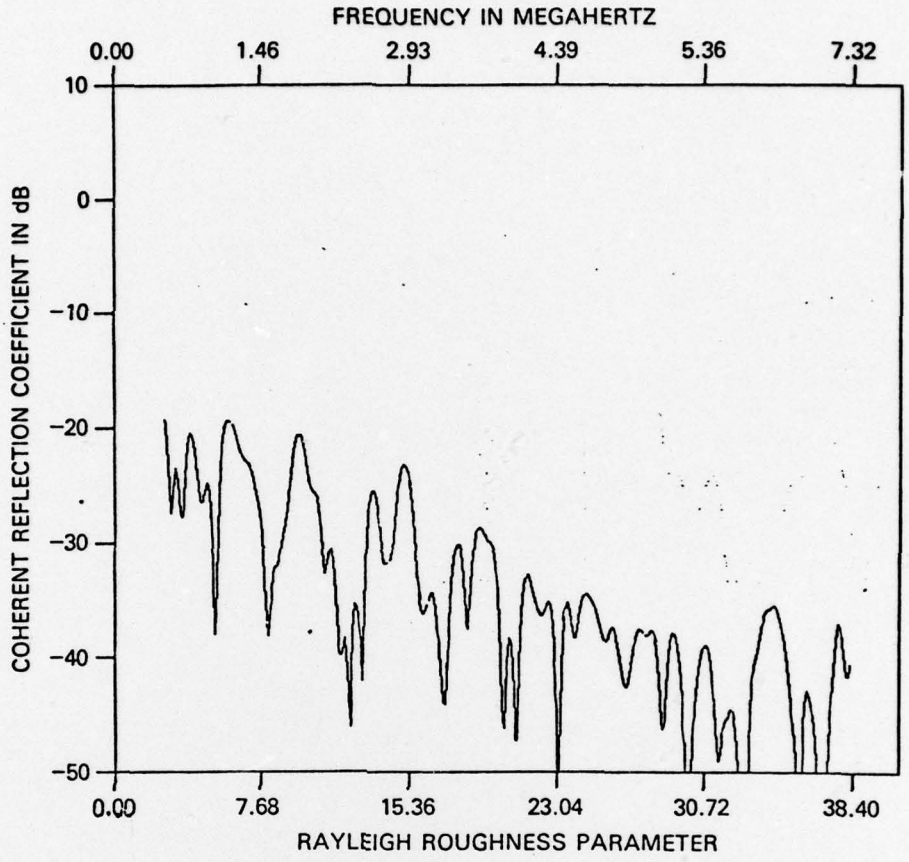

Fig. 11 Coherent reflection coefficients for 5.0 MHz transducer obtained by transient pulse analysis are plotted against the Rayleigh roughness parameter for brass surface I. Effects of phase cancellations are dramatic.

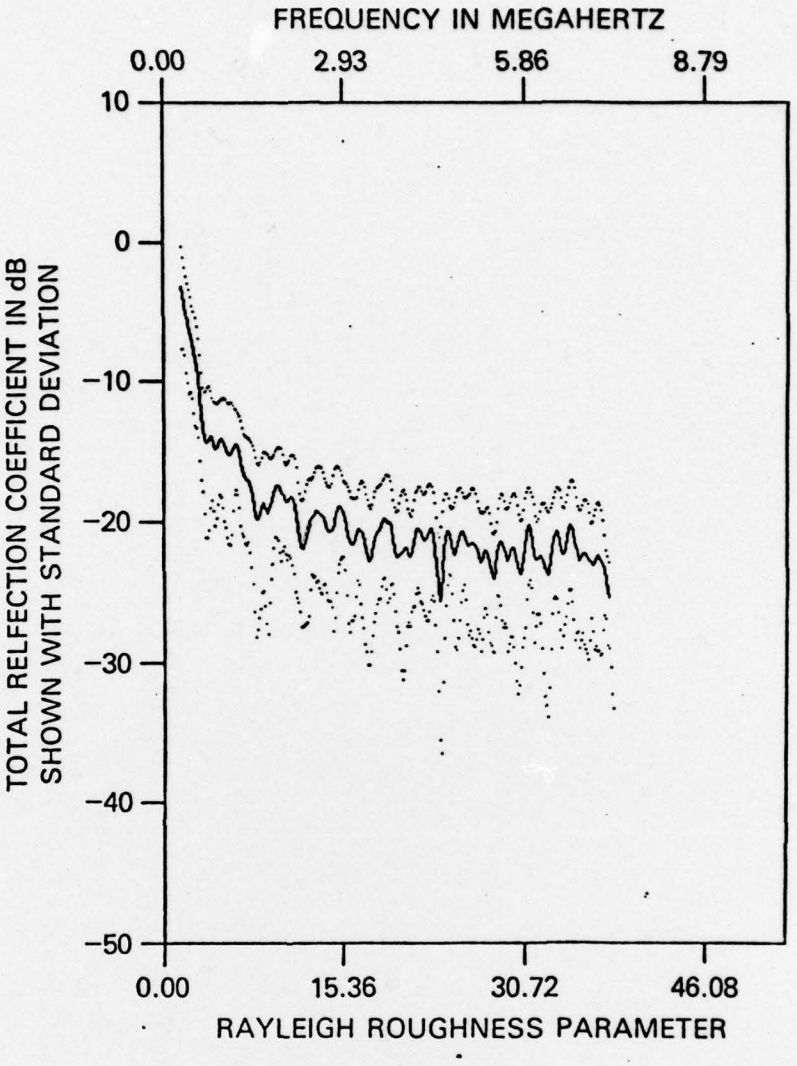

Fig. 12 Total reflection coefficients for 5.0 MHz transducer obtained by transient pulse analysis are plotted against the Rayleigh roughness parameter for brass surface I. The standard deviation for each data point brackets the mean curve.

UNCLASSIFIED

SECURITY CLASSIFICATION OF THIS PAGE (When Data Entered)

REPORT DOCUMENTATION PAGE	READ INSTRUCTIONS BEFORE COMPLETING FORM
1. REPORT NUMBER	2. GOVT ACCESSION NO.
3. RECIPIENT'S CATALOG NUMBER (9)	
4. TITLE (and Subtitle) (6) Rough Surface Acoustic Scattering and Scattering of Acoustic Waves from Rough Surfaces,	5. TYPE OF REPORT & PERIOD COVERED Informal final report,
	6. PERFORMING ORG. REPORT NUMBER
7. AUTHOR(s) (10) Susan K. Numrich and Earl Callen	8. CONTRACT OR GRANT NUMBER(s) NRL Problem 81S01-89 (15) N00014-77-C-0142
9. PERFORMING ORGANIZATION NAME AND ADDRESS Naval Research Laboratory, Code 8123 Washington, D. C. 20375 and American University, Washington D.C. 20016	10. PROGRAM ELEMENT, PROJECT, TASK AREA & WORK UNIT NUMBERS NR RR032-05-0142 611.53
11. CONTROLLING OFFICE NAME AND ADDRESS (11) Office of Naval Research, Code 461 Arlington, Virginia 22217	12. REPORT DATE 2 April 1979
	13. NUMBER OF PAGES 18
14. MONITORING AGENCY NAME & ADDRESS (if different from Controlling Office) (12) 21p.	15. SECURITY CLASS. (of this report) Unclassified
	15a. DECLASSIFICATION/DOWNGRADING SCHEDULE

16. DISTRIBUTION STATEMENT (of this Report)

Approved for public release; distribution unlimited.

(16) RR03205

17. DISTRIBUTION STATEMENT (of the abstract entered in Block 20, if different from Report)

(17) RR032050 1

18. SUPPLEMENTARY NOTES

19. KEY WORDS (Continue on reverse side if necessary and identify by block number)

Acoustics
Underwater acoustics
Sound scattering
Random surface scattering
Rough surface scattering

20. ABSTRACT (Continue on reverse side if necessary and identify by block number)

Measurements have been made of sound scattered in the specular direction by fixed rough surfaces. The surfaces used were physical realizations of computer generated topographies which corresponded to Gaussian distributions in height to within specified limits. Measurements were made in water using 0.5-, 1.0-, and 2.25-MHz transducers. Transient pulse analysis techniques were used to provide information about the scattered pulse over a wide range of frequencies. Comparisons are made with several theoretical models including a multiple scattering model. The scattered field is also

DD FORM 1 JAN 73 1473 EDITION OF 1 NOV 65 IS OBSOLETE S/N 0102-LF-014-6601

Encl: (2) to NRL ltr 8132-71:SKN:jw

927 65 p

20. illustrated by means of schlieren visualization.